Earthquakes and Structures, *Vol. 13, No. 4 (2017) 397-407*
DOI: https://doi.org/10.12989/eas.2017.13.4.397

Parametric identification of the Bouc-Wen model by a modified genetic algorithm: Application to evaluation of metallic dampers

Ganping Shu[a] and Zongjing Li*[b]

School of Civil Engineering, Southeast University, Nanjing 210096, China

(Received September 23, 2017, Revised November 25, 2017, Accepted December 27, 2017)

Abstract. With the growing demand for metallic dampers in engineering practice, it is urgent to establish a reasonable approach to evaluating the mechanical performance of metallic dampers under seismic excitations. This paper introduces an effective method for parameter identification of the modified Bouc-Wen model and its application to evaluating the fatigue performance of metallic dampers (MDs). The modified Bouc-Wen model which eliminates the redundant parameter is used to describe the hysteresis behavior of MDs. Relations between the parameters of the modified Bouc-Wen model and the mechanical performance parameters of MDs are studied first. A modified Genetic Algorithm using real-integer hybrid coding with relative fitness as well as adaptive crossover and mutation rates (called RFAGA) is then proposed to identify the parameters of the modified Bouc-Wen model. A reliable approach to evaluating the fatigue performance of the MDs with respect to the Chinese Code for Seismic Design of Buildings (GB 50011-2010) is finally proposed based on the research results. Experimental data are employed to demonstrate the process and verify the effectiveness of the proposed approach. It is shown that the RFAGA is able to converge quickly in the identification process, and the simulation curves based on the identification results fit well with the experimental hysteresis curves. Furthermore, the proposed approach is shown to be a useful tool for evaluating the fatigue performance of MDs with respect to the Chinese Code for Seismic Design of Buildings (GB 50011-2010).

Keywords: parameter identification; metallic dampers; Bouc-Wen model; genetic algorithm

1. Introduction

The passive structural control technology has developed greatly with inventions and applications of multiple types of dampers since 1980s (Soong and Spencer 2002, Housner *et al*. 1997). Passive control devices can be generally categorized into six major types: metallic dampers (Lee *et al*. 2016, Chan *et al*. 2009, Tsai *et al*. 1993), friction dampers (Mualla and Belev 2002, Bhaskararao and Jangid 2006), viscoelastic dampers (Zhang and Soong 1992, Park 2001), viscous fluid dampers (Lin and Chopra 2002, Lee and Taylor 2010), tuned mass/liquid dampers (Rana and Soong 1998, Fujino *et al*. 1993) and electrorheological/magnetorheological dampers (Dyke *et al*. 1996, Xu *et al*. 2000). Due to advantages such as simple structure, stable performance and reasonable cost, metallic dampers (MDs) have gained extensive attention as a reliable approach for seismic vibration control of civil structures. Metallic dampers are normally incorporated into the frame structure with braces, as shown in Fig. 1. Thus, the story drift can be effectively imposed on the metallic damper and cause its plastic deformation which dissipates the input energy, while the frame and the brace remained undamaged during the earthquake.

With the significantly increasing demand for engineering application of metallic dampers, a standard and an approach to evaluating the performance of metallic dampers are in great need. It is noted that the strength and stiffness of metallic dampers tend to deteriorate under cyclic loading due to fatigue damage. The Chinese Code for Seismic Design of Buildings (GB 50011-2010) proposed a standard to ensure the fatigue performance of metallic dampers, which requires that the metallic dampers should be able to endure a qualification test of at least 30 repeated cycles under their designed displacement amplitude. Meanwhile, the variation of the main design criteria should remain within 15% before and after the test. The main mechanical performance parameters, i.e. the elastic stiffness K_d, the plastic stiffness K_d', the yield displacement u_{dy} and the yield force F_{dy} are considered to be the essential factors of the above-mentioned design criteria. Therefore, the key to evaluating the fatigue performance of metallic dampers is to identify the mechanical performance parameters before and after the consecutive 30 cycles.

The hysteretic behavior of the metallic damper within a structural system can be mathematically described by a hysteresis model. Various types of metallic dampers have been theoretically and experimentally studied over the last two decades (Tsai *et al*. 1993, Tehranizadeh 2001, Chan *et al*. 2009, Dusicka *et al*. 2010, Li *et al*. 2013, Han *et al*. 2014, Deng *et al*. 2015, Lee *et al*. 2016, Ji *et al*. 2016). However, different patterns of metallic dampers share the same types of hysteresis models, including bilinear model

*Corresponding author
E-mail: lzjcivil@163.com
[a]Professor
E-mail: sgp0818@vip.sina.com
[b]Ph.D. Student
E-mail: lzjcivil@163.com

ISSN: 2092-7614 (Print), 2092-7622 (Online)

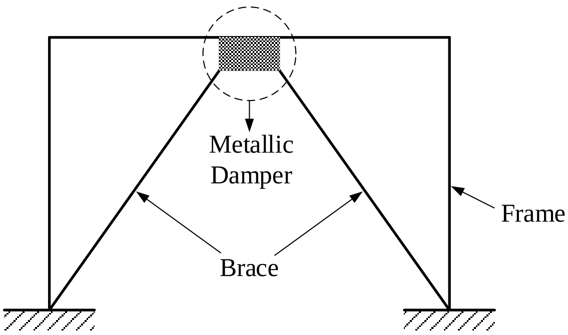

Fig. 1 Layout of frame-brace-MD system

(Chen *et al.* 2006), Ramberg-Osgood model (Sireteanu *et al.* 2014) and Bouc-Wen model (Chan *et al.* 2009, Sireteanu *et al.* 2014), among which the Bouc-Wen model is generally considered to be the most suitable class of hysteresis model for metallic dampers. The Bouc-Wen model was first proposed by Bouc(1967) and later generalized by Wen(1976). The traditional Bouc-Wen model includes 6 parameters and involves a differential equation, which makes the parameter identification complicated. Moreover, the traditional Bouc-Wen model is functionally redundant (Ma *et al.* 2004). In order to obtain the mechanical performance parameters of the metallic dampers through the Bouc-Wen model, the model needs to be modified in terms of eliminating the redundant parameter, and the relations between the model parameters and the performance parameters need to be uncovered.

The Genetic Algorithm as a powerful optimization tool, has been used in several studies to identify the Bouc-Wen model parameters over the past few years (Ismail *et al.* 2009). Liu *et al.* (2011) and Ha *et al.* (2006) adopted the standard real-coded Genetic Algorithm to identify the parameters of Bouc-Wen model for magnetorheological and piezoelectric dampers/actuators. Charalampakis and Koumousis (2008) proposed a modified Genetic Algorithm named "GAHC", which was a combination of Sawtooth GA and Greedy Ascent Hill Climbing, and Kwok *et al.* (2007) developed the "computationally-efficient GA" by incorporating the selection operator into the crossover operator to reduce the computational complexity of the identification algorithm. Kyprianou *et al.* (2001) and Ma *et al.* (2006) used "Differential Evolution Algorithm" for identification of the Bouc-Wen model parameters, which was similar to the real-coded Genetic Algorithm. In this study, in order to further enhance the efficiency of the identification, the Relative Fitness Adaptive Genetic Algorithm (RFAGA) is proposed, which modifies the standard Genetic Algorithm by incorporating real-integer hybrid coding, relative fitness, adaptive crossover and mutation rates and elitism strategy. Moreover, a more reasonable approach to estimate the parameter range before identification of the Bouc-Wen model is proposed, which can greatly enhance the efficiency of the identification as well. Based on the RFAGA, an approach to evaluating the fatigue performance of the metallic damper is proposed which consists of four stages, with the first complete cycle as Phase I to identify its initial mechanical performance parameters, the consecutive 30 cycles as Phase II as requested in the Chinese Code for Seismic Design of Buildings (GB 50011-2010), a smaller half cycle as Phase III to eliminate the residual plastic deformation, and the last complete cycle as Phase IV to identify its final mechanical performance parameters. Then the initial and final values of the mechanical performance parameters are compared to check if the degradation of each parameter remains within 15%, as suggested in the Chinese Code for Seismic Design of Buildings (GB 50011-2010).

The rest of this paper is organized as follows. In Section 2, a brief description is given to the modified Bouc-Wen model. The relations between the parameters of modified Bouc-Wen model and the mechanical performance parameters of the metallic damper are studied in Section 3. Relative Fitness Adaptive Genetic Algorithm (RFGA) is proposed to implement parameter identification of the modified Bouc-Wen model in Section 4, based on which the approach to evaluating the fatigue performance of the MDs with respect to the Chinese Code for Seismic Design of Buildings (GB 50011-2010) is developed and verified by experimental test data in Section 5. A conclusion is finally drawn in Section 6.

2. Modified Bouc-Wen model

The traditional standard Bouc-Wen model describes the restoring force in a hysteresis system in the following form (Wen 1976, Ma *et al.* 2004)

$$F = \alpha ku + (1-\alpha)kz \tag{1}$$

$$\dot{z} = A\dot{u} - \beta|\dot{u}|z|z|^{exp-1} - \gamma\dot{u}|z|^{exp} \tag{2}$$

where F is the restoring force, u is the displacement, z is the internal hysteresis variable. k controls the initial tangent stiffness, α controls the ratio of post-yield to pre-yield stiffness. A, β and γ are nondimensional parameters that control the shape of the hysteresis loop, while exp is a positive scalar that decides the smoothness of the transition from elastic to plastic response. The overdot represents derivative with respect to time t. In addition, the initial value for z is 0, i.e., $z(0)=0$.

Eq. (2) is normally a first-order nonlinear differential equation (unless exp=1). Thus, for most cases, no explicit expression can be given for parameter identification of the Bouc-Wen model. Moreover, the traditional Bouc-Wen model is functionally redundant (Ma *et al.* 2004). As a result, a specific Bouc-Wen hysteresis curve may correspond to multiple different parameter vectors. A drawback to this property is that identification procedures that use input-output data cannot determine the parameters of the Bouc-Wen model.

Ma *et al.* (2004) proposed a simple and effective alternative to remove the redundancy by setting A=1. Consequently, Eq. (2) can be modified as

$$\dot{z} = \dot{u} - \beta|\dot{u}|z|z|^{exp-1} - \gamma\dot{u}|z|^{exp} \tag{3}$$

Thus, the modified Bouc-Wen model is described by Eqs. (1) and (3). Instead of 6 parameters (A, k, α, β, γ, exp)

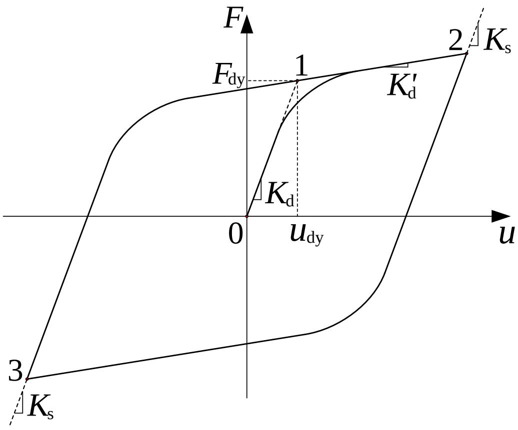

Fig. 2 Hysteresis loops described by the Bouc-Wen model

in the traditional Bouc-Wen model, the modified Bouc-Wen model has only 5 parameters (k, α, β, γ, exp). Meanwhile, the redundant parameter has been removed in model, so that parameter identification can be implemented directly based on the modified Bouc-Wen model.

3. Mechanical performance parameters of metallic dampers

Typical hysteresis loops of metallic dampers described by the Bouc-Wen model are shown in Fig. 2. Point 0 is the origin. Point 2 and 3 correspond to the positive and negative designed displacement amplitude of the metallic damper respectively. Point 1 is defined as the 'apparent yield point', which is the intersection of the elastic tangent line and the plastic tangent line. Displacement and restoring force corresponding to point 1 are defined as the yield displacement u_{dy} and yield force F_{dy}. The slopes of line $\overline{01}$ and $\overline{12}$ are defined as the initial elastic stiffness K_d and the plastic stiffness K_d'. (u_{dy}, F_{dy}, K_d, K_d') are the main mechanical performance parameters of the metallic damper, which are the crucial indexes in the evaluation of metallic dampers. Additionally, Point 2 and 3 are also defined as the 'shift point' at which the loading direction changes, i.e., the sign of the velocity $\dot{u}$ changes. Slope of the curve immediately after the 'shift point' is defined as the shift stiffness K_s. The relations between the above-stated performance parameters and the Bouc-Wen model parameters need to be studied first.

Dividing Eq. (3) by $\dot{u}$ yields

$$\frac{dz}{du} = 1 - \beta \frac{|\dot{u}|}{\dot{u}} z |z|^{exp-1} - \gamma |z|^{exp} \tag{4}$$

By solving Eq. (4), it reveals that the model is able to simulate softening system (i.e. the slope of the hysteresis curve decreases as |z| increases) with $\beta+\gamma>0$, and hardening system (i.e. the slope of the hysteresis curve increases as |z| increases) with $\beta+\gamma<0$, as shown in Fig. 3. Due to yielding of the metal material, the hysteresis loops for metallic dampers normally indicate a softening system.

For softening systems, $|z|$ reaches a maximum value z_m by setting Eq. (4) to zero. For $\dot{u}>0$ and $z>0$, or $\dot{u}<0$ and $z<0$, it gives

$$z_m = \left(\frac{1}{\beta+\gamma}\right)^{\frac{1}{exp}} \tag{5}$$

In the initial state, i.e., t=0, combining Eq. (3), $u(0)=0$ and $z(0)=0$, we get the initial slope of z

$$\left.\frac{dz}{du}\right|_{t=0} = 1 \tag{6}$$

According to Eqs. (5)-(6), when the system initiates in a positive direction, i.e., $\dot{u}>0$ and $z>0$, or in a negative

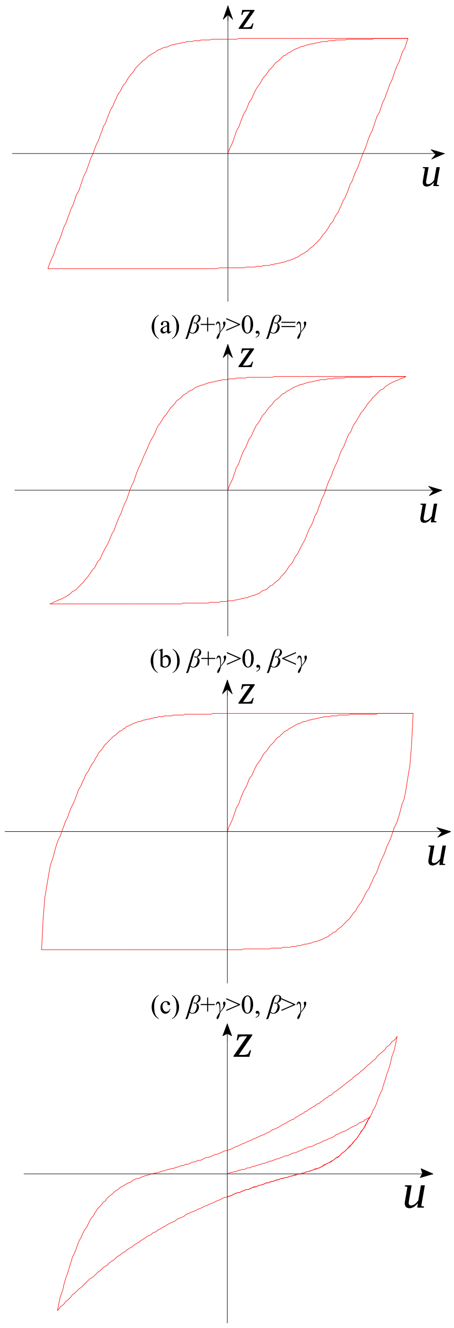

(a) $\beta+\gamma>0$, $\beta=\gamma$

(b) $\beta+\gamma>0$, $\beta<\gamma$

(c) $\beta+\gamma>0$, $\beta>\gamma$

(d) $\beta+\gamma<0$, $\beta>\gamma$

Fig. 3 Hysteresis shapes for z with different β and γ

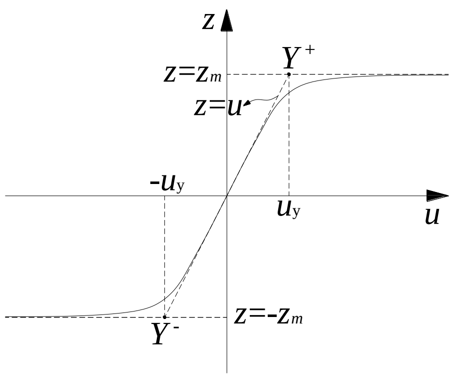

Fig. 4 *z*-*u* curves

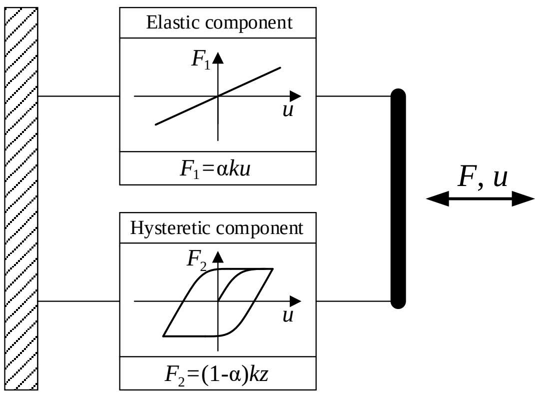

Fig. 5 Schematic of the Bouc-Wen model

direction, i.e., $\dot{u}<0$ and z<0, the relation between z and u is shown in Fig. 4, where points Y^+ and Y^- are the intersection of the initial tangent line z=u and the ultimate bounds $z=\pm z_m$, i.e., the equivalent yield points in the z-u curves. Thus the equivalent yield displacement in the z-u curves is

$$u_y = z_m \tag{7}$$

According to Eq. (1), the restoring force F can be taken as the parallel combination of an elastic linear part $F_1=\alpha ku$ and a hysteretic nonlinear part $F_2=(1\text{-}\alpha)kz$, as shown in Fig. 5. Thus, the yield displacement in the F-u hysteresis system is equal to the equivalent yield displacement in the z-u curves, which gives

$$u_{dy} = u_y = z_m = \left(\frac{1}{\beta+\gamma}\right)^{\frac{1}{exp}} \tag{8}$$

Combining Eqs. (4), (5) and (8), we get the yield force

$$F_{dy} = \alpha k u_{dy} + (1\text{-}\alpha)kz_m = k\left(\frac{1}{\beta+\gamma}\right)^{\frac{1}{exp}} \tag{9}$$

Differentiate Eq. (4) with respect to dispalcement u

$$\frac{dF}{du} = \alpha k + (1-\alpha)k\frac{dz}{du} \tag{10}$$

Thus, when t=0, combining Eqs. (6), (10) and $u(0)$=0, we get the initial elastic stiffness

$$K_d = \left.\frac{dF}{du}\right|_{u=0} = k \tag{11}$$

Differentiate Eq. (1) with respect to displacement with $u\to\infty$, it follows

$$\left.\frac{dF}{du}\right|_{u\to\infty} = \alpha k + (1-\alpha)k\left.\frac{dz}{du}\right|_{u\to\infty} \tag{12}$$

The slope of the internal hysteresis variable z decreases to 0 as u approaches infinity, as shown in Fig. 4, which gives

$$\left.\frac{dz}{du}\right|_{u\to\infty} = 0 \tag{13}$$

By substituting Eq. (13) into Eq. (12), we get the post-yield stiffness

$$K_d' = \alpha k \tag{14}$$

As shown in Fig. 2, $sign(\dot{u}z)<0$ is satisfied after both the positive and negative shift points. Therefore, Eq. (3) can be revised as

$$\frac{dz}{dt} = \frac{du}{dt}(1+(\beta-\gamma)|z|^{exp}) \tag{15}$$

By substituting Eq. (5) into Eq. (15), we get the slope of the z-u curve immediately after the shift points

$$\frac{dz}{du} = 1+\frac{\beta-\gamma}{\beta+\gamma} \tag{16}$$

Combining Eqs. (10) and (16), we get the shift stiffness

$$K_s = k\left[1+\frac{(1-\alpha)(\beta-\gamma)}{\beta+\gamma}\right] \tag{17}$$

By comparing Eqs. (11) and (17), the relation between K_d and K_s is as follows

$$\begin{cases} K_s > K_d \ , & \text{if } \beta>\gamma \\ K_s = K_d \ , & \text{if } \beta=\gamma \\ K_s < K_d \ , & \text{if } \beta<\gamma \end{cases} \tag{18}$$

4. Parameter Identification by RFGA

Genetic Algorithms (GAs) as a powerful and popular stochastic search algorithm were first proposed by Holland (1975) based on the idea of Darwin's evolution theory, and then developed by Goldberg (1989). GAs find the global optimal solution in complex multidimensional search space by simultaneously evaluating multiple points in the parameter space. They require only information concerning the quality of the solution and do not require linearity in the parameters. Thus, GAs are widely used to solve optimization, parameter identification and many other problems in various domains.

In this study, a modified form of Genetic Algorithms named Relative Fitness Adaptive Genetic Algorithms

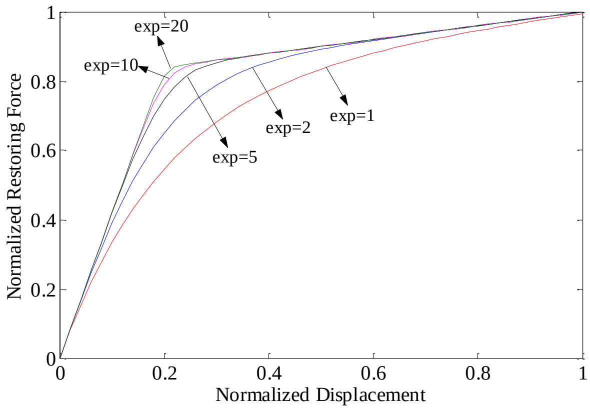

Fig. 6 Influence of *exp* to the hysteresis shape

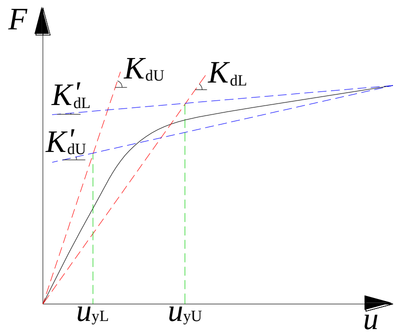

Fig. 7 Estimation of upper and lower bounds for K_d, K_d' and u_{dy}

(RFAGA) is adopted for parameter identification of the modified Bouc-Wen model, featuring relative fitness function as well as adaptive crossover and mutation probabilities. Major steps of parameter identification in this study are elaborated as follows.

4.1 Parameter ranges

Before starting the parameter identification with GA, the value range of each parameter needs to be confirmed, which composes the entire search space of interest. Upper and lower bounds of the parameters are given as

$$\text{UB}=(k_{\text{U}}, \alpha_{\text{U}}, \beta_{\text{U}}, \gamma_{\text{U}}, exp_{\text{U}}) \tag{19a}$$

$$\text{LB}=(k_{\text{L}}, \alpha_{\text{L}}, \beta_{\text{L}}, \gamma_{\text{L}}, exp_{\text{L}}) \tag{19b}$$

Generally, significantly large initial ranges could be set for the parameters to encompass all possibilities, and then narrowed down by a few trials of the parameter identification process. However, this could be time-consuming and sometimes misleading. In order to enhance the efficiency of the identification, the bounds of the parameters need to be narrowed down to more specific ranges.

exp governs the smoothness of the transition from elastic to plastic response, and is usually set as a positive integer in common practice. As *exp* goes near 10 or above, the Bouc-Wen curve almost turns into a bilinear model (see Fig. 6), which is rarely seen in the hysteresis loops of metallic dampers. Thus, for most cases, practical bounds of *exp* could be set as exp_{L}=1 and exp_{U}=10, i.e.,

$$1 \le exp \le 10 \tag{20}$$

Given that K_{d} and K_{d}' represents the slope of the elastic response curve and the slope of the plastic response curve respectively, and the intersection of the elastic and plastic response curves is the 'apparent yield point', which corresponds to the yield displacement u_{dy}, the upper and lower bounds of K_{d}, K_{d}' and u_{dy} could be estimated from the test hysteresis curves as shown in Fig. 7, i.e.,

$$K_{\text{dL}} \le K_{\text{d}} \le K_{\text{dU}} \tag{21}$$

$$K_{\text{dL}}' \le K_{\text{d}}' \le K_{\text{dU}}' \tag{22}$$

$$u_{\text{dyL}} \le u_{\text{dy}} \le u_{\text{dyU}} \tag{23}$$

By substituting Eqs. (11) and (14) into inequalities (21) and (22), it gives the bounds for k and α as $k_{\text{U}} = K_{\text{dU}}$, $k_{\text{L}} = K_{\text{dL}}$, $\alpha_{\text{U}} = \dfrac{K'_{\text{dU}}}{K_{\text{dL}}}$, $\alpha_{\text{L}} = \dfrac{K'_{\text{dL}}}{K_{\text{dU}}}$, i.e.,

$$K_{\text{dL}} \le k \le K_{\text{dU}} \tag{24}$$

$$\frac{K'_{\text{dL}}}{K_{\text{dU}}} \le \alpha \le \frac{K'_{\text{dU}}}{K_{\text{dL}}} \tag{25}$$

By substituting Eq. (8) into inequality (23), it gives

$$\frac{1}{b} \le \beta + \gamma \le \frac{1}{a} \tag{26}$$

where a and b are defined as

$$a = \left(u_{dyL}\right)^{exp_0} \tag{27a}$$

$$b = \left(u_{\text{dyU}}\right)^{exp_0} \tag{27b}$$

in which exp_0 is an initial guess of the parameter *exp* within the range defined in inequality (20) depending on the actual smoothness of transition in the hysteresis loop. According to previous theoretical and experimental investigation results (Tsai *et al*. 1993, Chen *et al*. 2006, Chan *et al*. 2009, Dusicka *et al*. 2010, Li *et al*. 2013, Han *et al*. 2014, Sireteanu *et al*. 2014, Deng *et al*. 2015, Ji *et al*. 2016, Lee *et al*. 2016), the shift stiffness K_{s} is normally quite close to the initial elastic stiffness K_{d} for metallic dampers. Consequently, based on Eqs. (17) and (18), the difference between β and γ is small. Thus, with inequality (26), the initial bounds for β and γ can be set as

$$\frac{1}{2b} \le \beta \le \frac{1}{2a} \tag{28}$$

$$\frac{1}{2b} \le \gamma \le \frac{1}{2a} \tag{29}$$

According to the above stated equations and inequalities, ranges of the five model parameters (k, α, β, γ, *exp*) can be established. Additionally, the initial setting of exp_0 or the bounds for β and γ can be further revised based on the results of a trial implementation of the parameter identification if needed.

4.2 Real-integer hybrid coding

Traditional Genetic Algorithms use binary coding to represent values of variables. However, in parameter identification, it would need excessive length of binary coding strings to achieve desired precision, which may seriously affect the efficiency of the algorithm. As aforementioned, the parameters k, α, β and γ are real numbers, while the parameter *exp* is usually set as a positive integer. Therefore, the real-integer hybrid coding is adopted here instead of the traditional binary coding. The model parameter set is encoded into a hybrid real-integer string $w=(w_1, w_2, w_3, w_4, w_5)$, where w_1, w_2, w_3, w_4 are real numbers representing the values of k, α, β and γ respectively, while w_5 remains a positive integer representing the value of *exp*.

4.3 Objective function and fitness function

The aim of the parameter identification is to minimize the error between the test data and the simulation data. Thus, the objective function for this problem could be set as the root-mean-squared-error (*RMSE*) as follows

$$e_i = \sqrt{\frac{1}{n}\left(\sum_{j=1}^{n}(F_j^{\text{sim}} - F_j^{\text{test}})^2\right)} \tag{30}$$

where e_i is the objective function of the ith chromosome in the population. n is the total number of data points. F_j^{sim} is the simulated restoring force of the jth point, while F_j^{test} is the tested restoring force of the jth point. Note that e_i has the same unit with the restoring force. Individuals with less error should possess higher fitness values, and thus have larger chances to be selected, which means the objective function and the fitness function should be inversely related. In addition, the fitness function should always remain non-negative. For such instances, fitness function is commonly set as

$$f_i = C_{\max} - e_i \tag{31}$$

where f_i is the fitness function of the ith chromosome in the population. $C_{\max}$ is a constant representing the upper bound of the objective function. However, $C_{\max}$ cannot be determined for the objective function described in Eq. (30) in this study. Thus, as an alternative, Relative Fitness Genetic Algorithm (RFGA) is adopted in this study, whose fitness function is described as

$$\begin{cases} f_i = e_{\max} - e_i \quad , \text{ if } \; e_{\max} \neq e_{\min} & \text{(32a)} \\ f_i = c \quad (c \neq 0) \;\; , \text{ if } \; e_{\max} = e_{\min} & \text{(32b)} \end{cases}$$

where $e_{\max}$ and $e_{\min}$ are the maximum and minimum objective function value in the population, respectively. c is a nonzero constant. Thus, the chromosomes with less error will have higher fitness values, and thus have larger chances to be selected.

4.4 Selection

Selection is a genetic operator that makes more copies of better individual chromosomes in a new population. Selection is usually the first operator applied on population. By evaluating the chromosomes with the fitness function, good individuals in a population are selected and forms a mating pool. Thus, in selection operation the process of natural selection cause those individuals that encode better solutions to produce copies more frequently.

There are various methods for the selection operator, such as Roulette Wheel Selection, Rank Selection, Steady State Selection and Tournament Selection. In this study, the Roulette Wheel method is adopted as the selection operator. The probability of the ith chromosome to be selected is

$$p_i = \frac{f_i}{\sum_{j=1}^{n} f_j} \tag{33}$$

4.5 Crossover and mutation

Crossover and mutation are two important procedures that direct the search for solutions by exploitation and exploration. The crossover operator aims to refine the best solution found so far, while the mutation operator is devoted to search for solution spaces that have not been covered. The two-point arithmetic crossover method and single point mutation method are employed in this study.

In particular, modified adaptive crossover and mutation rates are adopted in this study. Srinivas (1994) proposed a theory of adaptive probabilities of crossover and mutation in GA, in which p_c and p_m are not fixed but dependent on the fitness value. Chromosomes with fitness value below average will be crossed or mutated more frequently. Furthermore, in the case that the average fitness shifts to a higher value, the proposed mechanism automatically favors a higher crossover and mutation rate. Thus, a trade-off between exploitation of the optimum solution and exploration of the solution space is maintained. However, in his theory, the crossover and mutation rates of the chromosomes with the highest fitness values are close to 0, which is unfavorable in the early stage of the evolution. To overcome the above stated problem, the crossover rate P_{c} and mutation rate P_{m} in this study are modified as shown in Eqs. (34)-(35).

$$P_{\text{c}} = \begin{cases} P_{\text{c1}} - \dfrac{(P_{\text{c1}} - P_{\text{c2}})(f' - f_{\text{avg}})}{f_{\max} - f_{\text{avg}}} & (f' \geq f_{\text{avg}}) \\ P_{\text{c1}} & (f' < f_{\text{avg}}) \end{cases} \tag{34}$$

$$P_{\text{m}} = \begin{cases} P_{\text{m1}} - \dfrac{(P_{\text{m1}} - P_{\text{m2}})(f - f_{\text{avg}})}{f_{\max} - f_{\text{avg}}} & (f \geq f_{\text{avg}}) \\ P_{\text{m1}} & (f < f_{\text{avg}}) \end{cases} \tag{35}$$

where P_{c1} and P_{c2} are the upper and lower bounds of the probability of crossover respectively. P_{m1} and P_{m2} are the

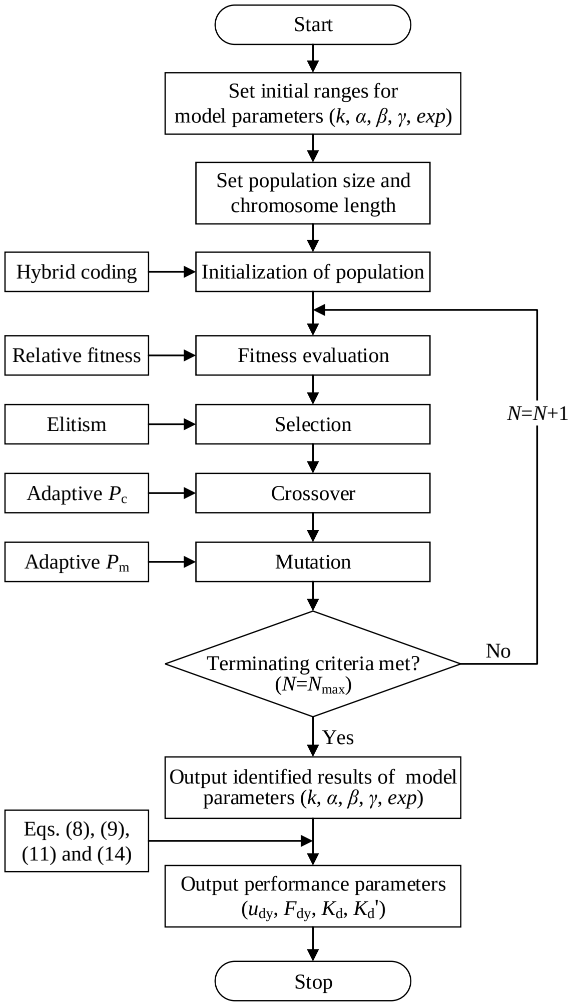

Fig. 8 Flow chart of the parameter identification process

upper and lower bounds of the probability of mutation respectively. f_{max} is the maximum fitness value of the population, while f_{avg} is the average fitness value of the population. f' is the larger of the fitness value of the chromosomes to be crossed, while f is the fitness value of the chromosome to be mutated. According to Eqs. (34)-(35), the crossover rate of the chromosome with the highest fitness value is P_{c2}, and the mutation rate of the chromosome with the highest fitness value is P_{m2}.

4.6 Elitism strategy

During iterations of GA, good individuals can be lost when crossover or mutation results in weaker offspring, which may influence the efficiency of the searching process. Elitism strategy (Rudolph 1994) is adopted within the selection operator to overcome the above stated problem. By copying one or several fittest individuals into the next generation, survival of the best chromosomes in subsequent generations are ensured. As a result, elitism can enhance the performance of GA significantly. In this study, the best individual of the *i*th generation is copied directly into the (*i*+1)th generation, replacing the worst individual of the (*i*+1)th generation.

4.7 Terminating criteria

There are many possible ways to terminate the GA iteration. For example, the GA may terminate after the expiry of a fixed number of generations. Alternatively, by monitoring the change on the fitness value, the GA may terminate when there are no more significant fitness improvements within a fixed number of iterations. In this study, the GA iteration stops when a selected number of generations (N_{max}) is reached.

After the parameters of normalized Bouc-Wen model are identified, the main performance parameters of the metallic damper could be obtained by Eqs. (8), (9), (11) and (14).

The complete identification process can be expressed by the flow chart shown in Fig. 8, according to which the identification process is finally implemented via MATLAB code.

5. Experimental verification

Based on the parameter identification method developed in Section 4, the procedures for fatigue performance evaluation of metallic dampers with respect to the Chinese Code for Seismic Design of Buildings (GB 50011-2010) is proposed as follows.

The loading protocol of the qualification test is shown in Fig. 9, which can be divided into 4 stages. The key time points are also shown in the figure, where t_0, t_1, t_2 and t_3 are the time when each stage begins; t_4 is the time when the loading protocol ends; t_2' is the time when the loading reverses direction in phase III; t_3' is the time when the loading first reverses direction in phase IV. In phase I, the tested metallic damper sample is loaded for the first full cycle to obtain its initial mechanical performance parameters ($u_{dy0}, F_{dy0}, K_{d0}, K'_{d0}$) using the parameter identification method presented in Fig. 8. Then in phase II, it is loaded for 30 consecutive cycles under designed displacement amplitude $\pm u_m$ as requested in the Chinese Code for Seismic Design of Buildings (GB 50011-2010). Phase III is implemented to eliminate the residual plastic deformation. The hysteresis curves of the metallic damper in Phase III is show in Fig. 10. As shown, the loading path is A→B→O→C in Fig. 10, where point A correspond to t_2 in Fig. 9; point B correspond to t_2' in Fig. 9; point O correspond to t_3 in Fig. 9; point C correspond to t_3' in Fig. 9. Thus, the hysteresis curve may return to the origin point at the end of Phase III, and Phase IV may start from the origin point. In phase IV, it is loaded for the last full cycle to obtain its final mechanical performance parameters ($u_{dy1}, F_{dy1}, K_{d1}, K'_{d1}$) using the parameter identification method presented in Fig. 8. Finally, the variations of the mechanical performance parameters between the first cycle and the last cycle are checked. If the variations are all within 15%, the tested metallic damper sample is qualified, or else it is disqualified. Additionally, it is suggested that we use the test data of a complete cycle for the identification to account for the variance within a complete cycle because the hysteresis loops are not always perfectly

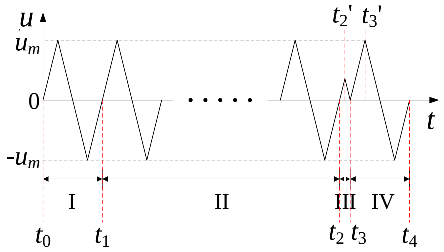

Fig. 9 Loading protocol of the qualification test

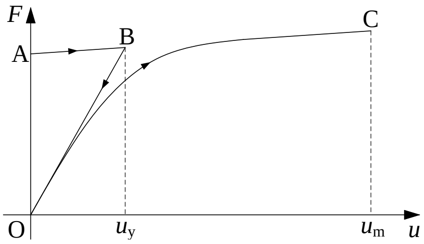

Fig. 10 Hysteresis curve between t_2 and t_3'

centrosymmetric. However, if the hysteresis loops are almost perfectly centrosymmetric, identification using the data of a quarter in the complete cycle (i.e., "the monotonic loading" part) can be an alternative to reduce the time cost for the identification.

It is to be noted that the Bouc-Wen model adopted here does not explicitly simulate the process of fatigue behavior of the metallic dampers. It is used to identify the mechanical performance parameters before and after the 30 consecutive cycles separately, and the fatigue performance is finally evaluated by comparing the identification results.

A new type of metallic damper was developed and tested in Southeast University (Li *et al*. 2013). A symmetric test setup was adopted as shown in Fig. 11, which is a widely accepted loading scheme for metallic dampers (De la Llera *et al*. 2004, Shih and Sung 2005). 6 identical core plates of the tested metallic damper were loaded simultaneously by an MTS actuator. In order to evaluate the fatigue performance of the metallic damper, the loading protocol given in Fig. 9 was adopted. The loading displacement amplitude was set as $\pm u_m$=±30 mm (i.e., the designed displacement amplitude). Force and displacement were measured and recorded during the test, from which the hysteresis loops were drawn as shown in Fig. 12. The maximum strain on the MD core plates reached about 0.018 during the cyclic loading test (corresponding to the maximum displacement amplitude u_m=30 mm).

The aforementioned RFAGA is adopted to identify the parameters of the modified Bouc-Wen model using the force-displacement data of the first and the last cycle in the test, respectively. The population size is set as n=40, maximum number of iterations N_{max}=100, the upper and lower bounds of crossover probability P_{c1}=0.9 and P_{c2}=0.5, the upper and lower bounds of mutation probability P_{m1}=0.1 and P_{m2}=0.02. The parameter ranges are first estimated by the method proposed in Section 4.1, which gives the lower bounds as (k_L, α_L, β_L, γ_L, exp_L)=(40, 0.005, 0.05, 0.05, 1), and the upper bounds as (k_U, α_U, β_U, γ_U, exp_U)=(100, 0.03, 0.40, 0.40, 10) for the identification of both the first and the

(a) Picture

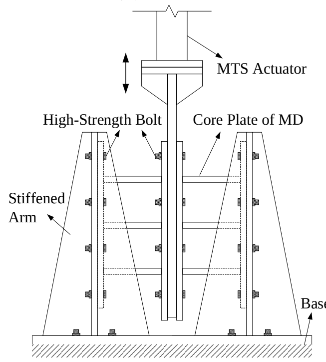

(b) Schematic

Fig. 11 Test setup

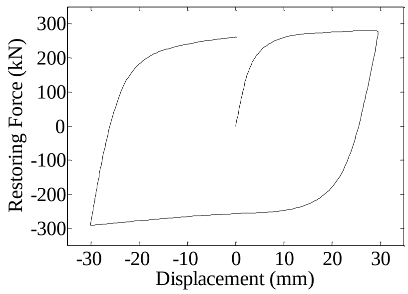

(a) First cycle

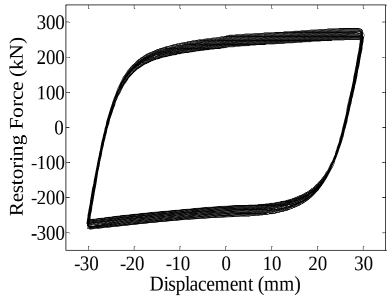

(b) 30 consecutive cycles

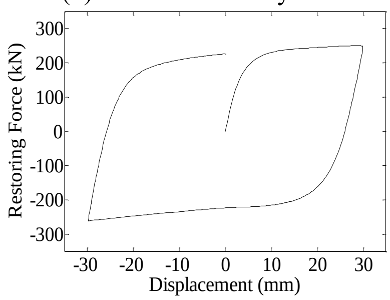

(c) Last cycle

Fig. 12 Hysteresis loops of metallic damper

Table 1 Identification results

	Modified Bouc-Wen model parameters					MD mechanical performance parameters				*RMSE* (kN)	Relative error*
	k	*α*	*β*	*γ*	*exp*	K_d (kN/mm)	K_d' (kN/mm)	u_{dy} (mm)	F_{dy} (kN)		
First cycle	72.47	0.0142	0.1364	0.1446	1	72.47	1.03	3.56	257.90	8.94	3.07%
Last cycle	65.18	0.0150	0.1396	0.1453	1	65.18	0.98	3.51	228.70	7.38	2.83%
Variation			—			10.06%	4.99%	1.40%	11.32%	—	

*Relative error: The ratio of *RMSE* to the maximum restoring force of the hysteresis loop, i.e., $RMSE / F_{max}$

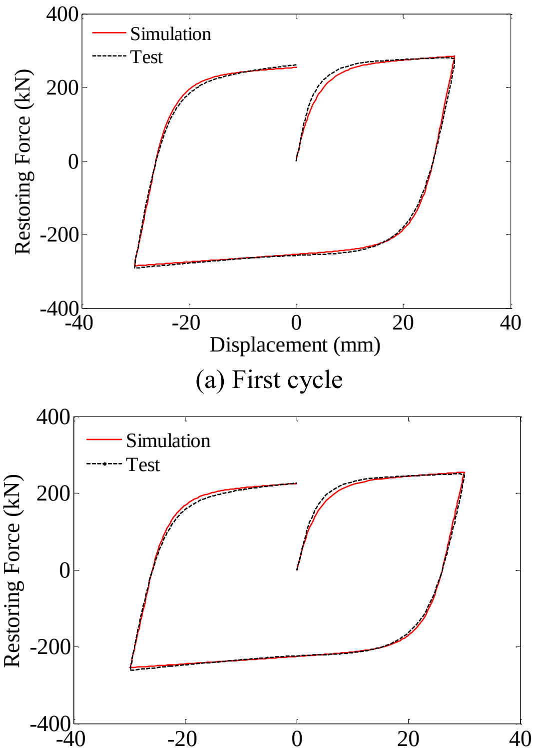

(a) First cycle

(b) Last cycle

Fig. 13 Experimental hysteresis loop vs. simulated hysteresis loop

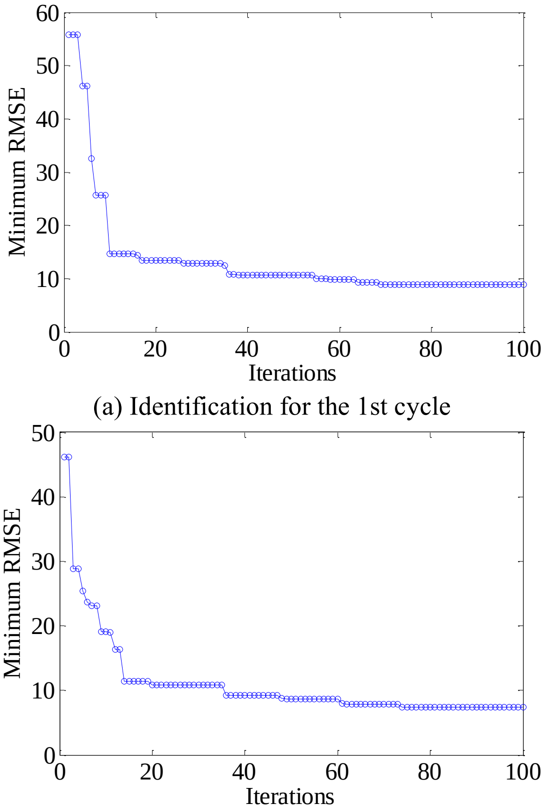

(a) Identification for the 1st cycle

(b) Identification for the last cycle

Fig. 14 Convergence curves of RFAGA

last cycle. Then 40 initial guesses are randomly generated within the ranges, which represent the first generation in the Genetic Algorithm. After the model parameters (k, α, β, γ, exp) are identified, the performance parameters (u_{dy}, F_{dy}, K_d, K_d') can be calculated by Eqs. (8), (9), (11) and (14).

The identification results are listed in Table 1. As shown, the variations of mechanical performance parameters between the first cycle and the last cycle are all within 15%, which satisfies the requirements in the Chinese Code for Seismic Design of Buildings (GB 50011-2010), and therefore qualifies the tested metallic damper sample in terms of fatigue performance. The *RMSE*s of the final solution is 8.94kN and 7.38kN for identification of the first cycle and the last cycle respectively, and the relative errors are within 5%, which indicates that the errors between the experimental data and the simulation results can be minimized to a reasonable level.

Furthermore, the same identified parameter values of *exp* can be found in the first and the last cycles. This is because the parameter *exp* determines the smoothness of transition from elastic to plastic response, and the smoothness of transition almost remained unchanged between the first and the last cycles. Besides, the search range for *exp* is set as positive integers within [1, 10] as aforementioned. Thus, it is reasonable that the identified values of *exp* remained unchanged. Additionally, as shown in Table 1, the identified parameter values of β and γ are quite close for the first and the last cycles, while a noticeable reduction in the identified parameter values of k is observed between the first and the last cycles. The reason is that k is the key parameter which controls the stiffness and strength, while β and γ controls the yield placement according to the equations given in Section 3. Noticeable degradation of stiffness and strength can be observed in Fig. 12, while the yield placement remained almost unchanged. Thus, it is reasonable that the variations of β and γ are smaller, while the variation of k is larger in the identification results between the first and the last cycles.

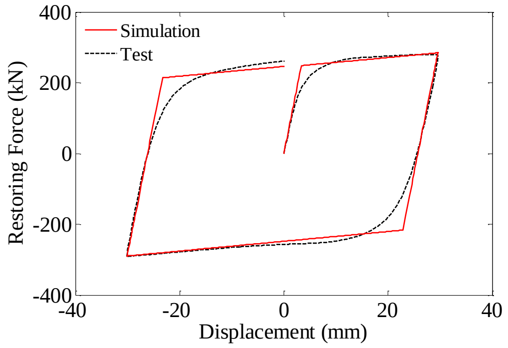

Fig. 15 Experimental hysteresis loop vs. simulated bilinear hysteresis loop

Comparison of hysteresis loops by test data and by simulation model based on identification results is shown in Fig. 13. As shown, the simulated curves fit well with the experimental data, which proves the validity of the proposed parameter identification method. Convergence curves of RFAGA are shown in Fig. 14, which indicates the RFAGA used in the parameter identification is able to converge quickly within 100 iterations. The time consumption of the parameter identification using the proposed RFAGA is around 10 minutes, which is an acceptable time cost for engineering application.

Additionally, in order to clarify the difference between identification using the bilinear model and the Bou-Wen model, test data of the first cycle is used for the bilinear model identification as an example, in which the same objective function (RMSE) and algorithm (RFAGA) are used. The identified bilinear model is shown in Fig. 15. By comparing Fig. 13(a) and Fig. 15, the identified Bouc-Wen model fits the test data quite well, while the identified bilinear model exhibits noticeably larger deviation from the test data. Moreover, the *RMSE* of the bilinear model identification is 23.81 kN, which is significantly larger than that of the Bouc-Wen model identification. The main reason can be explained that the Bouc-Wen model is able to simulate the smooth transition from elastic to plastic response, which makes it more adaptive to the actual hysteresis curves of metallic dampers, while the bilinear model simplifies the transition to a sharp point. Thus, it is more reasonable and convincing to evaluate the fatigue performance of metallic dampers using the Bouc-Wen model.

6. Conclusions

This paper has presented an effective approach for parameter identification of the modified Bouc-Wen model and its application to evaluation of fatigue performance for metallic dampers. The major findings are summarized as follows:

• Relations between the modified Bouc-Wen model parameters and the mechanical performance parameters of metallic dampers are uncovered. Consequently, the performance parameters can be obtained after the model parameters are identified.

• A new method based on Relative Fitness Adaptive Genetic Algorithm (RFAGA) is proposed to identify the model parameters using the experimental test data. It is shown that RFAGA used in the identification is able to converge quickly, and the simulated hysteresis curves based on the identification results match well with the test hysteresis curves, which proves the effectiveness and efficiency of the identification method.

• The procedures for evaluating the fatigue performance of metallic dampers are proposed based on the aforementioned findings, and verified by a qualification test. The approach is shown to be a useful and reliable tool for evaluation of metallic dampers with respect to the Chinese Code for Seismic Design of Buildings (GB 50011-2010).

Acknowledgments

The financial support from the National Key Technology R&D Program of China during the 12th Five-Year Plan Period under Grant No. 2012BAJ13B01 is gratefully acknowledged.

References

Bhaskararao, A.V. and Jangid, R.S. (2006), “Seismic analysis of structures connected with friction dampers”, *Eng. Struct.*, **28**(5), 690-703.

Bouc, R. (1967), “Forced vibration of mechanical systems with hysteresis”, *Proceedings of the 4th Conference on Nonlinear Oscillation*, Prague, Czechoslovakia, September.

Chan, R.W.K., Albermani, F. and Williams, M.S. (2009), “Evaluation of yielding shear panel device for passive energy dissipation”, *J. Constr. Steel Res.*, **65**(2), 260-268.

Charalampakis, A.E. and Koumousis, V.K. (2008), “Identification of Bouc-Wen hysteretic systems by a hybrid evolutionary algorithm”, *J. Sound Vibr.*, **314**(3), 571-585.

Chen, Z., Ge, H. and Usami, T. (2006), “Hysteretic model of stiffened shear panel dampers”, *J. Struct. Eng.*, **132**(3), 478-483.

Chinese Code for Seismic Design of Buildings (GB 50011-2010), *Ministry of Housing and Urban-Rural Construction of People’s Republic of China*, Beijing, China.

De La Llera, J.C., Esguerra, C. and Almazán, J.L. (2004), “Earthquake behavior of structures with copper energy dissipators”, *Earthq. Eng. Struct. Dyn.*, **33**(3), 329-358.

Deng, K., Pan, P., Li, W. and Xue, Y. (2015), “Development of a buckling restrained shear panel damper”, *J. Constr. Steel Res.*, **106**, 311-321.

Dusicka, P., Itani, A.M. and Buckle, I.G. (2010), “Cyclic behavior of shear links of various grades of plate steel”, *J. Struct. Eng.*, **136**(4), 370-378.

Dyke, S.J., Spencer, B.F., Sain, M.K. and Carlson, J.D. (1996), “Modeling and control of magnetorheological dampers for seismic response reduction”, *Smart Mater. Struct.*, **5**(5), 565-575.

Fujino, Y., Sun, L., Pacheco, B.M. and Chaiseri, P. (1993), “Tuned liquid damper (TLD) for suppressing horizontal motion of structures”, *J. Eng. Mech.*, **118**(10), 2017-2030.

Goldberg, D.E. (1989), *Genetic Algorithms in Search, Optimization, and Machine Learning*, Addison-Wesley New York, U.S.A.

Ha, J., Kung, Y., Fungc, R. And Hsien, S.C. (2006), “A comparison of fitness functions for the identification of a piezoelectric hysteretic actuator based on the real-coded genetic algorithm", *Sens*. *Actuat*. *A*: *Phys*., **132**(2), 643-650.

Han, Q., Jia, J., Xu, Z., Bai, Y. and Song, N. (2014), "Experimental evaluation of hysteretic behavior of rhombic steel plate dampers", *Adv*. *Mech*. *Eng*., **2014**, 1-8.

Holland, J.H. (1975), *Adaptation in Natural and Artificial Systems*, University of Michigan Press, Ann Arbor, Michigan, U.S.A.

Housner, G., Bergman, L.A., Caughey, T.K., Chassiakos, A.G., Claus, R.O., Masri, S.F., Skelton, R.E., Soong, T.T., Spencer, B.F. and Yao, J.T. (1997), "Structural control past, present, and future", *J*. *Eng*. *Mech*., **123**(9), 897-971.

Ismail, M., Ikhouane, F. and Rodellar, J. (2009), "The hysteresis Bouc-Wen model, a survey", *Arch*. *Comput*. *Meth*. *Eng*., **16**(2), 161-188.

Ji, X., Wang, Y., Ma, Q. and Okazaki, T. (2016), "Cyclic behavior of very short steel shear links", *J*. *Struct*. *Eng*., **142**(2), 04015114.

Kwok, N.M., Ha, Q.P., Nguyen, M.T., Li, J. and Samali, B. (2007), "Bouc-Wen model parameter identification for a MR fluid damper using computationally efficient GA", *ISA Trans*., **46**(2), 167-179.

Kyprianou, A., Worden, K. and Panet, M. (2001), "Identification of hysteresis systems using the differential evolution algorithm", *J*. *Sound Vibr*., **248**(2), 289–314.

Lee, C.H., Lho, S.H., Kim, D.H., Oh, J. and Ju, Y.K. (2016), "Hourglass-shaped strip damper subjected to monotonic and cyclic loadings", *Eng*. *Struct*., **119**, 122-134.

Lee, D. and Taylor, D.P. (2010), "Viscous damper development and future trends", *Struct*. *Des*. *Tall Spec*. *Build*., **10**(5), 311-320.

Li, Z.J., Huang, Z. and Li, A.Q. (2013), "Theoretical and experimental study of new type of mild steel plate damper with opening", *J*. *Southeast Univ*., **43**(2), 392-397.

Lin, W.H. and Chopra, A.K. (2002), "Earthquake response of elastic SDF systems with non-linear fluid viscous dampers", *Earthq*. *Eng*. *Struct*. *Dyn*., **31**(9), 1623-1642.

Liu, Y., Yang, S., Liao, Y.Y. and Zhang, G.N. (2011), "Parameter identification of Bouc-Wen model for MR damper based on genetic algorithm", *J*. *Vibr*. *Shock*, **30**(7), 261-265.

Ma, F., Ng, C.H. and Ajavakom, N. (2006), "On system identification and response prediction of degrading structures", *Struct*. *Contr*. *Health Monitor*., **13**, 347-364.

Ma, F., Zhang, H., Bockstedte, A., Foliente, G.C. and Paevere, P. (2004), "Parameter analysis of the differential model of hysteresis", *J*. *Appl*. *Mech*., **71**(3), 342-349.

Mualla, I.H. and Belev, B. (2002), "Performance of steel frames with a new friction damper device under earthquake excitation", *Eng*. *Struct*., **24**(3), 365-371.

Park, S.W. (2001), "Analytical modeling of viscoelastic dampers for structural and vibration control", *J*. *Sol*. *Struct*., **38**(44), 8065-8092.

Rana, R. and Soong, T.T. (1998), "Parametric study and simplified design of tuned mass dampers", *Eng*. *Struct*., **20**(3), 193-204.

Rudolph, G. (1994), "Convergence analysis of canonical genetic algorithms", *IEEE Trans*. *Neur*. *Netw*., **5**(1), 96-101.

Shih, M. and Sung, W. (2005), "A model for hysteretic behavior of rhombic low yield strength steel added damping and stiffness", *Comput*. *Struct*., **83**(12-13), 895-908.

Sireteanu, T., Mitu, A.M., Giuclea, M. and Solomon, O. (2014), "A comparative study of the dynamic behavior of Ramberg-Osgood and Bouc-Wen hysteresis models with application to seismic protection devices", *Eng*. *Struct*., **76**, 255-269.

Soong, T.T. and Spencer, B.F. (2002), "Supplemental energy dissipation: State-of-the-art and state-of-the-practice", *Eng*. *Struct*., **24**, 243-259.

Srinivas, M. and Patnaik, L.M. (1994), "Adaptive probabilities of crossover and mutation in genetic algorithms", *IEEE Trans*. *Syst*. *Man Cybernet*., **24**(4), 656-667.

Tehranizadeh, M. (2001), "Passive energy dissipation device for typical steel frame building in Iran", *Eng*. *Struct*., **23**(6), 643-655.

Tsai, K.C., Chen, H.W., Hong, C.P. and Su, Y.F. (1993), "Design of steel triangular plate energy absorbers for seismic-resistant construction", *Earthq*. *Spectr*., **9**(3), 505-528.

Wen, Y.K. (1976), "Method for random vibration of hysteretic systems", *J*. *Eng*. *Mech*., **102**(2), 249-263.

Xu, Y.L., Qu, W.L. and Ko, J.M. (2000), "Seismic response control of frame structures using magnetorheological/electrorheological dampers", *Earthq*. *Eng*. *Struct*. *Dyn*., **29**(5), 557-575.

Zhang, R. and Soong, T.T. (1992), "Seismic design of viscoelastic dampers for structural applications", *J*. *Struct*. *Eng*., **118**(5), 1375-1392.

KT